Shipboard PEBB Cooling Strategies

S. Yang*, J. S. Chalfant†, J. C. Ordonez*, J. A. Khan‡, C. Li‡, I. Cvetkovic§,
J. V. C. Vargas*, M. B. Chagas*, Y. Xu§, R. P. Burgos§, D. Boroyevich§
*Center for Advanced Power Systems
Florida State University, Tallahassee, Florida 32310
E-mail: syang@caps.fsu.edu, ordonez@caps.fsu.edu, jvargas@caps.fsu.edu
†Sea Grant Design Laboratory
Massachusetts Institute of Technology, Cambridge, Massachusetts 02139
E-mail: chalfant@mit.edu
‡Department of Mechanical Engineering
University of South Carolina, Columbia, South Carolina 29208
E-mail: khan@cec.sc.edu, li01@cec.sc.edu
§Center for Power Electronics Systems
Virginia Tech, Blacksburg, Virginia 24061
E-mail: igorc@vt.edu, rolando@vt.edu, dushan@vt.edu

Abstract—**We discuss herein several cooling strategies applicable to shipboard Power Electronics Building Blocks (PEBBs), namely the PEBB 1000 and a notional PEBB 6000 currently under development, subject to the following design goals and constraints: (1) small and lightweight package (i.e., high power density); (2) easy swapability achieved by minimizing any connections requiring sailor intervention for connecting or disconnecting; and (3) any thermal solution must be able to cool not only a single PEBB unit, but also multiple units placed in close proximity to one another when combined to make up a converter. For the PEBB 1000 application, air cooling is most likely sufficient to meet the needs, and several arrangements of fin structures were investigated. On the other hand, air cooling, water cooling, and water cooling with a dry interface all have potential for meeting the cooling demand of an envisioned PEBB 6000 and warrant further investigation. In any case, the localized heat generated within the PEBB will require significant spreading to a larger surface area for subsequent transfer out of the PEBB.**

I. INTRODUCTION

The increasing power demand and complexity of an all-electric ship have forced its constituents to operate near their design limits. In particular, the quest to achieve greater capabilities from compact and resilient energy systems stresses the need for effective thermal management strategies under design and operational constraints faced by an all-electric ship. Power electronic building blocks (PEBBs), for example, are converters that provide robust control and hardware for power conversion and management in an extremely power-dense package. Despite their high power-conversion efficiency, the heat dissipated by these PEBBs poses serious thermal challenges. The thermal aspects of shipboard PEBBs hence deserve a closer scrutiny to complement the enhanced electrical performance by providing proper cooling in all conceivable scenarios.

Traditional PEBB cooling strategies include heat sinks, direct liquid cooling, and heat pipes, and [1] presents a thorough review of both traditional and emerging electronics cooling techniques that are applicable to PEBBs. Nonetheless, the design requirements and limitations imposed on shipboard PEBBs—particularly in pursuit of shipboard power corridor [2] to which the PEBBs may be allocated—can restrict the application of conventional cooling methods. The concept of power corridor presents additional design constraints such as compactness (i.e., smaller space for cooling) and modularity (i.e., minimal piping and direct contact between a PEBB and its stack; quick disconnects) for PEBBs. As a result, we explore herein several cooling strategies applicable to shipboard PEBBs, namely PEBB 1000 and PEBB 6000 currently under development at the Center for Power Electronics Systems at Virginia Tech (CPES/VT).

II. NOTIONAL SHIPBOARD PEBBS

The next-generation PEBB features modular and distributed controls, integrated protection, low sensitivity to parasitics and electromagnetic interference, and integrated redundancy for high reliability. Moreover, the intelligent gate driver with current and voltage sensing allows for faster overcurrent protection and control. Fig. 1a depicts the SiC-based PEBB 1000 designed and assembled at CPES/VT [3], whereas Fig. 1b illustrates the possible PEBB 6000 prototype currently under development at CPES/VT which could potentially resemble the expanded form of PEBB 1000 [4].

The PEBB 1000 interfaces 1 kV DC bus operating at 100 kW, 100-kHz, and with 98% conversion efficiency, whereas the envisioned PEBB 6000 hardware prototype under development would be for 6-kV DC bus operating at 1 MW,

---

This material is based upon research supported by, or in part by, the U.S. Office of Naval Research (ONR) under award number ONR N00014-16-1-2956 Electric Ship Research and Development Consortium; ONR N00014-16-1-2945 Incorporating Distributed Systems in Early-Stage Set-Based Design of Navy Ships; and by the National Oceanic and Atmospheric Administration (NOAA) under Grant Number NA14OAR4170077 - MIT Sea Grant College Program. Any opinions, findings, and conclusions or recommendations are those of the authors and do not necessarily reflect the views of ONR or NOAA.

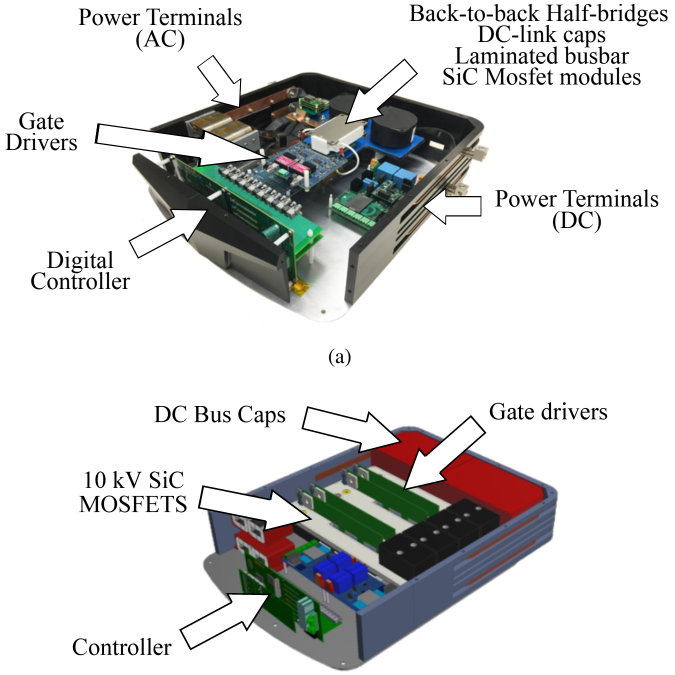

(a)

(b)

Fig. 1. (a) PEBB 1000 assembly and (b) envisioned PEBB 6000 hardware prototype currently under development at CPES/VT [4].

20-100 kHz, and with approximately 99% efficiency [4]. The total heat dissipated by PEBB 1000 is about 2 kW (1 kW on each side) while that of an envisioned PEBB 6000 would be approximately 10 kW according to its anticipated power conversion efficiency. Furthermore, local heat fluxes in these PEBBs can reach up to 10^5 $\mathrm{W/m^2}$; thus, effective heat distribution paths from local heat sources to PEBB surfaces are necessary to reduce the hot spot temperature. Additional details of the PEBB 1000 and notional PEBB 6000 under development can be found in Refs. [3]–[6].

The maximum allowable junction temperature to prevent thermal runaway is device-specific. For MOSFETs with high switching frequency, a junction temperature of about 200°C is deemed acceptable [7]. The onset of thermal runaway is dictated by the interplay of conduction losses, switching losses, ambient or heat sink temperature, and the thermal conductance of the cooling system. In particular, the SiC MOSFET for PEBB 1000 exhibits an operating junction temperature of 150°C and case and storage temperature of up to 125°C (1.7 kV, 300 A Wolfspeed/CREE SiC MOSFET). PEBB 6000 is envisioned to feature an SiC MOSFET with an operating temperature of 200°C (10 kV, 240 A Wolfspeed/CREE SiC MOSFET) [4].

III. THERMAL MANAGEMENT STRATEGIES

The vision is that the PEBB will be a universal, programmable converter that can be used individually or combined in series or parallel with other PEBBs to increase voltage or current as necessary, thus creating uni-directional or bi-directional converters for a wide range of applications, power levels and voltage levels; see, for example, Fig. 2. In this vision, individual PEBB units are of a size that can be easily carried by a sailor through a ship and can be hot-swapped in and out of a converter and easily latched into place with no external connections that must be made up individually.

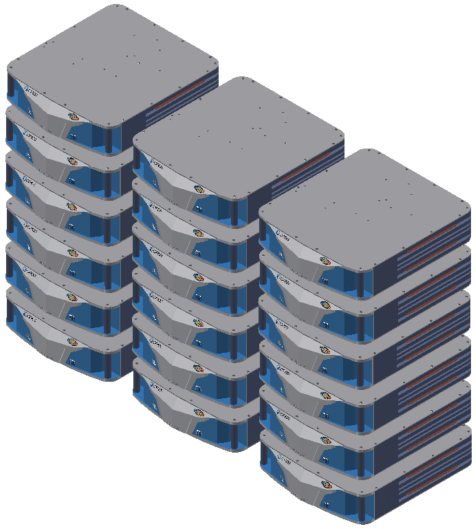

Fig. 2. PEBBs can be combined in series or parallel as required to increase voltage or current [6].

This vision places some interesting constraints on the thermal management of the PEBB. First, the portability requirement encourages a small and light weight package, i.e., high power density. Second, it is undesirable to have water in proximity to the electrical components, thus limiting the cooling medium options. Third, the voltage levels of the units demand electrical isolation in the cooling path as well as the electrical path. Fourth, the swapability requirement discourages any connections requiring sailor intervention for connecting or disconnecting, beyond pushing the unit into place and latching it down. Finally, any thermal solution must be able to cool not only a single unit, but also multiple units placed in close proximity to one another when combined to make up a converter.

The thermal management of PEBBs can be divided into three aspects, as shown in Fig. 3: (1) internal cooling, (2) thermal interface (PEBB envelope), and (3) external cooling. The internal cooling ensures proper heat dissipation from the local heat sources (e.g., MOSFET) to the thermal interface via diffusion and natural convection. Similarly, the thermal interface plays a key role in providing necessary heat flow paths from the PEBB interior to its exterior for an even heat distribution and increased heat transfer to the external cooling medium. The external cooling of PEBBs is typically achieved with forced air or liquid while more sophisticated methods such as heat pipes and microchannels may be employed to spread heat to new areas or to increase heat transfer across an interface.

The dominant heat source in the considered PEBB designs would be the SiC MOSFET module. For example, Fig. 4

shows the layout of a MOSFET array in an envisioned PEBB 6000 hardware prototype wherein approximately 10 kW of heat would be generated in the tan area. The heat transfer coefficient, h, is then obtained as

$$h = \frac{\dot{Q}}{A\Delta T}, \tag{1}$$

where $\dot{Q}$ is the heat transferred, A is the heat transfer area, and ΔT is the difference in temperature between the surfaces. The effective heat transfer area of each MOSFET module in both PEBBs would be approximately 4.8 in × 2.45 in. Assuming a ΔT of 35 K, the required convective heat transfer for PEBB 1000, which houses two MOSFET modules, is 3.8×10^3 W/m^{2}K, whereas $h = 6.3 \times 10^3$ W/m^{2}K for the envisioned PEBB 6000 prototype illustrated in Fig. 1b.

If the heat were to be spread to the gray area in Fig. 4, measuring 11 in (27.94 cm) by 12 in (30.48 cm), the required h for the notional PEBB 6000 under development would decrease by nearly 50% (i.e., 3.4×10^3 W/m^{2}K). Furthermore, h could be reduced by another 58% if the heat were spread evenly to the notional 17.3 in (43.94 cm) × 19.3 in (49.02 cm) PEBB cover. Hence such a reduction in the required heat transfer coefficient highlights the importance of large and uniform heat distribution in the thermal interface to achieve the same level of cooling effect with a smaller h.

Fig. 5 summarizes the range of overall heat transfer coefficients for different cooling techniques and heat transfer fluids. According to the figure, forced air convection is entirely appropriate for cooling the PEBB 1000, achieving a $\Delta T \approx 35$ K. The PEBB 6000, which is envisioned as a scaled-up version of PEBB 1000, is expected to dissipate significantly more heat from potentially about the same size package. This would then require either a much larger heat transfer area and change in temperature, or cooling methods with a much higher heat transfer coefficient in the neighborhood of 10^3 W/m^{2}K or above. Methods that can achieve a sufficiently high heat transfer coefficient include direct liquid cooling (e.g., microchannels), heat pipes, impinging jets, etc. The cooling system design complexity, however, typically increases along with the overall heat transfer coefficient.

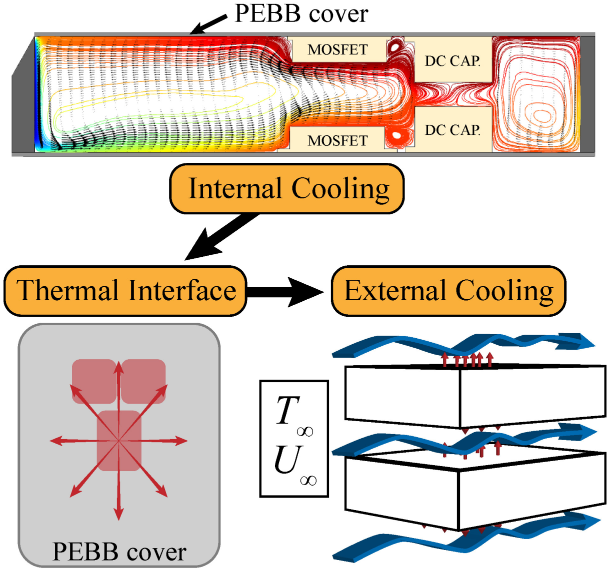

Fig. 3. Three aspects of PEBB cooling.

Table I lists the estimated minimum heat transfer area and mass flow rate required by each representative PEBB cooling method displayed in Fig. 5 for $\Delta T = 35$ K and nominal heat transfer coefficient. The heat transfer area in Table I can be obtained from Eq. (1) while the mass flow rate $\dot{m}$ is computed as

$$\dot{m} = \frac{hA\Delta T}{c_p \Delta T_f}, \tag{2}$$

in which ΔT_f is the fluid temperature difference between the inlet and outlet and c_p is the fluid specific heat.

In the remainder of this section we briefly explore the advantages and disadvantages of several options for external cooling of PEBB units.

A. Air Cooling

A wide variety of liquid cooling solutions have been proposed for thermal management of electronics, e.g., solid-state cooling, impinging jet, immersion cooling, etc. [8], and they outperform air cooling solutions from a purely thermal standpoint. However, safety, simple maintenance, reduced manpower, and ease of interchangeability justify exploring solutions for which no direct liquids are utilized. Air cooling has the advantages of no manual connections required upon installation, no liquid present, and no electrical conductivity in

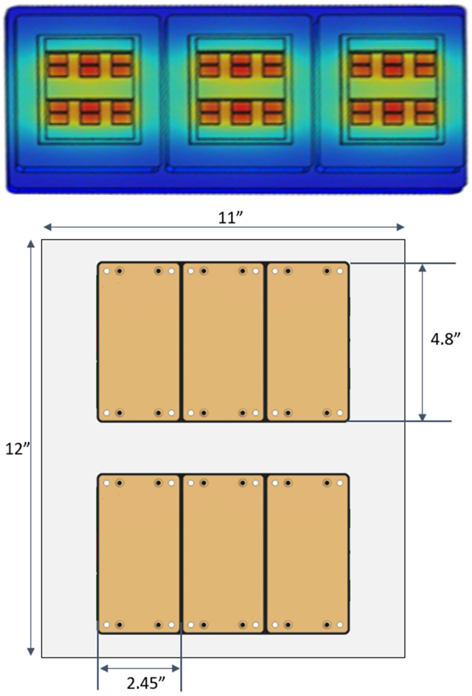

Fig. 4. Cooling configuration for an envisioned PEBB 6000 hardware prototype currently under development at CPES/VT.

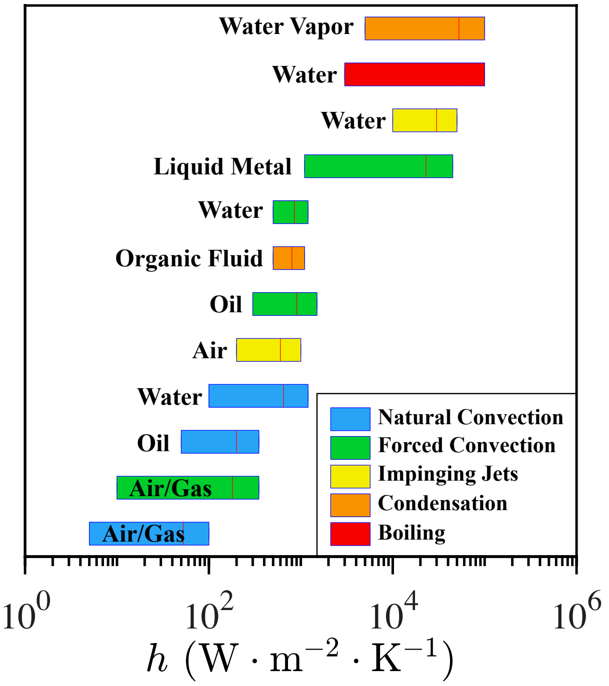

Fig. 5. Range of overall heat transfer coefficients for different fluids and cooling techniques.

TABLE I
MINIMUM HEAT TRANSFER AREA AND MASS FLOW RATE REQUIRED BY THE RESPECTIVE COOLING METHOD, ASSUMING ΔT = 35K

Method	ΔT_f (K)	h $(\mathrm{W/m^2K})$	A (m^2)	$\dot{m}$ (kg/s)
PEBB 1000 ($\dot{Q} = 2$ kW)				
Air, external	2	100	0.57	1.00
Water, direct	2	1000	0.06	0.24
Water, dry	2	910	0.06	0.24
Impinging air	10	800	0.07	0.20
Envisioned PEBB 6000 under development ($\dot{Q} \approx 10$ kW)				
Air, external	10	100	2.86	1.00
Water, direct	10	1000	0.29	0.24
Water, dry	10	910	0.31	0.24
Impinging air	10	800	0.36	1.00

the cooling medium. The thermal interface would most likely be a finned surface, and would be integral to the PEBB, which may increase the size and weight of the PEBB beyond the desired limits.

1) PEBB 1000 Air Cooling: According to Table I, the PEBB 1000 would require extended surfaces if external air cooling is desired as the required area to achieve $\Delta T = 35$ K is 0.57 m^2 (or about 2.9 times larger than the sum of top and bottom surface areas). We thereby simulated different copper pin-fin configurations (number of pins and inlet air temperature and velocity) to verify the feasibility of cooling a PEBB 1000 with forced air as depicted in Fig. 6. The complete PEBB 1000 geometry with two MOSFET modules and capacitor banks were considered in the simulation while neglecting the internal natural convection. Furthermore, we varied the PEBB cover material between aluminum (Al) and copper (Cu) to quantify their heat-spreading effectiveness. The peak temperature observed with each configuration is given in Table II.

TABLE II
CONSIDERED PIN-FIN CONFIGURATIONS AND THE RESPECTIVE PEAK TEMPERATURE OF PEBB 1000

#	Fins?	U_∞ (m/s)	T_∞ (K)	Cover	N$_{fins}$	T_{max} (K)
1	N	10	279	Cu	None	406.7
2	N	5	279	Al	None	484
3	N	10	279	Al	None	438.5
4	Y	10	279	Al	5x5	413.9
5	Y	10	279	Al	15x15	372.3
6	Y	10	279	Cu	5x5	387.9
7	Y	5	279	Cu	15x15	384.2
8	Y	10	279	Cu	15x15	357.5
9	Y	5	293	Cu	15x15	397
10	Y	10	293	Cu	15x15	370.3

The MOSFET module achieved the peak temperature as it generated the most heat, and the PEBB cover served as a thermal interface that distributed heat across the plane as well as to the pins for enhanced cooling. The peak temperature decreased remarkably with a higher number of pins as well as with Cu cover since Cu has higher thermal conductivity than Al. According to Table II, forced air convection is apt for PEBB 1000 cooling especially with a Cu cover and increased heat transfer area. If the cover material as well as the inlet air conditions are restricted to Al and higher temperature and lower velocity, respectively, heat transfer area can be increased further by adding more fins or using alternative fin designs such as wavy or rectangular.

2) Envisioned PEBB 6000 Air Cooling: Using the temperature assumptions of Table I, the notional PEBB 6000 under development would require a surface area of 2.86 m^2 and a mass flow rate of 1 $\mathrm{kg/s}$. This large volume of air requires a large fan with a correspondingly large power requirement. The fan could be integral to the PEBB or part of the external structure in which the PEBB is mounted. Chilling the inlet air to a low temperature, such as 283 K, and assuming a higher heat transfer coefficient of 150 $\mathrm{W/m^2K}$ could be used to reduce both the mass flow rate and the area required. Using Eqs. (1) and (2) with a $\Delta T = 50$ K and $\Delta T_f = 15$ K yields a surface area of 1.33 m^2 and a mass flow rate of 0.67 $\mathrm{kg/s}$. This large surface area would require an extended fin structure, and the chilled inlet air would require a localized cooling system.

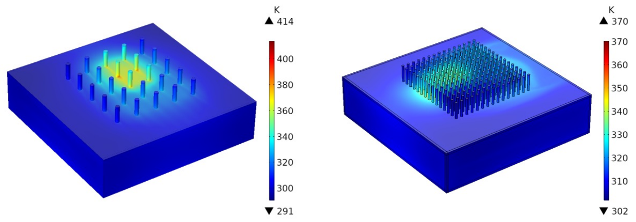

(a) 5 × 5

(b) 15 × 15

Fig. 6. Forced air-cooled PEBB 1000 with an extended surface.

B. Single-phase Liquid Cooling

Direct liquid cooling can be achieved by connecting flexible hoses to the individual PEBBs after inserting the PEBB into place in the power corridor. Direct-contact liquid cooling is much more efficient than air cooling with a much smaller thermal interface than air cooling for the same amount of heat, resulting in a smaller and lighter PEBB. De-ionized water or dielectric liquids can be used to eliminate electrical conductivity of the cooling medium and non-conductive connections can be used to eliminate electrical conductivity through the connections themselves. No-leak quick-disconnects are common in the marine environment, and the power corridor can be designed so that the quick disconnects are on the front of the unit, easily visible and separated from any electrical connections. If greater heat transfer is required, mini- or micro-channels can be implemented in the thermal interface within the PEBB.

The disadvantages of this method are that it violates the prohibition against manual connections, and it places circulating water in proximity to the electrical components, which is potentially problematic in view of a leak or some externally imposed damage. Further, the PEBBs would need to be drained down before removing, and would need to have air bled from the system when connecting.

C. External liquid cooling with a dry interface

External liquid cooling with a dry interface can be achieved by passing liquid through a cold plate in the power corridor; the cold plate is in contact with a solid surface of the PEBB unit as depicted in Fig. 7 and heat is transferred by conduction across these surfaces. The advantages of this methodology are that there are no manual external connections that must be made up, there is no liquid entering the PEBB, and electrical isolation can be ensured. However, there is contact resistance where the cold plate and the hot PEBB surface come in contact with one another, which can provide a significant barrier to heat transfer, especially in an environment with dirt and grit present.

The interface conductance comprises solid-solid conductance and gap conductance as $h = h_c + h_g$. Yovanovich and Antonetti proposed [9]

$$h_c = 1.25 k_s \frac{m}{\sigma} \left(\frac{P}{H} \right)^{0.95} \tag{3}$$

where $k_s = 2k_1k_2/(k_1 + k_2)$ is the harmonic mean thermal conductivity for solid 1 and solid 2. The ratio m/σ is typically in between $1/9\ \mu\text{m}^{-1}$ and $1/5\ \mu\text{m}^{-1}$ for smooth surfaces. P is the contact pressure and H is the microhardness of the softer material; both in N/m^2.

The gap conductance is given by

$$h_g = \frac{k_g}{Y + M} \tag{4}$$

where k_g for air is $0.032\ \text{W}/(\text{mK})$ at 100°C and

$$\frac{Y}{\sigma} = 1.185 \left[-\ln \left(3.132 \frac{P}{H} \right) \right]^{0.547}. \tag{5}$$

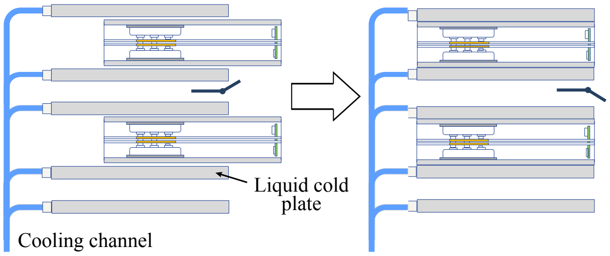

Fig. 7. Dry interface liquid cooling with a cold plate [6].

Here σ is the effective root mean square surface roughness, $\sigma = \sqrt{\sigma_1^2 + \sigma_2^2}$. $M \approx 0.1734\ \mu\text{m}$ is a gas parameter included to account for rarefied gas effects [10]. Table III lists the interface conductance of common materials [9], [11].

Heat transfer is improved when pressure is increased and when contact area is increased. The typical approach to increasing contact area is to apply a thermal grease; however, the grease would need to be cleaned off the surfaces whenever a unit is swapped out, requiring the sailor to reach into the space where other PEBBs are operating. Another approach would be to insert an interface pad which compresses and improves contact when the surfaces are placed together. Examples of interface materials include metal wools, polymer wools, or phase-changing polymers that are liquid when hot and dry when cool. These can improve heat transfer up to 30%. Contact area can also be increased through design of the interface profile.

Increasing contact pressure requires careful design of the mechanical support system; achieving uniform pressure across a large surface area is challenging. However, use of springs and flexible interfaces can assist in this endeavor.

D. Advanced Methods

Ongoing research in many locations is developing methodologies for higher heat-flux applications; examples include liquid-metal heat exchangers and phase-changing liquid jet impingement. These methods have the benefit of much higher heat flux, thus allowing a reduction in the surface area required for heat transfer; however, they introduce significant complexity in the support structure, and are most likely unnecessary for our needs.

TABLE III
TYPICAL INTERFACE CONDUCTANCES [11], [12]

Interface	h $(\text{W}/\text{m}^2\text{K})$
Ceramic – Ceramic	500 – 3,000
Ceramic – Metal	1,500 – 8,500
Graphite – Metal	3,000 – 6,000
Stainless Steel (SS) – SS	1,500 – 4,000
Copper – Copper	10,000 – 25,000
Iron – Al	4,000 – 40,000
Al – Al with grease ($\approx 100\ \text{kN}/\text{m}^2$)	$\approx 140,000$
SS – SS with grease ($\approx 3500\ \text{kN}/\text{m}^2$)	$\approx 250,000$

IV. HEAT SPREADERS

The previous section discussed the importance of thermal interface and its heat spreading effectiveness in reducing the hot spot temperature. As a result, we also explored various heat spreaders suitable for the considered PEBB designs, namely conductive serpentine cooling paths, heat sink, and heat pipes.

A. Serpentine Cooling Paths

Conductive serpentine cooling paths of different configurations (i.e., number of meanders as well as inlet and outlet locations along the PEBB perimeter) across the PEBB 1000 thermal interface were studied numerically to achieve more uniform temperature distributions [13]. The serpentine cooling path consists of a high thermal conductivity material capable of diffusing heat away from localized sources. Fig. 8 illustrates the serpentine cooling path concept described herein, and the temperature field across the PEBB cover is obtained by solving the Poisson's equation given as

$$k\nabla^2 T + \dot{Q}''' = 0. \qquad (6)$$

k in Eq. (6) is the thermal conductivity of the copper cooling path ($k = 400$ W/mK) or the aluminum cover ($k = 280$ W/mK) while $\dot{Q}'''$ is the volumetric heat generation rate. In our preliminary study, we fixed $T_c = 25$°C, $\dot{Q}''' = 100$ kW/m^3 in each component, and the path length was fixed at 3 times the PEBB side length.

Fig. 9 shows three distinct path configurations under consideration, and the maximum plate temperature (T_{max}) varies slightly with respect to the path configuration. Here T_{max} does not represent the maximum component temperature but that of the aluminum plate as the devices are not explicitly modeled yet; the junction temperature must therefore be higher than T_{max}. The preliminary numerical assessment alludes to the possibility of adopting serpentine cooling paths as heat spreaders especially for PEBB 1000, and detailed evaluation of various path layouts and quantification of their heat spreading effects is underway. In addition, the proposed serpentine cooling path model can be extended to study different liquid channel layouts by solving for fluid flow as well as heat pipe layouts by assuming an effective thermal conductivity.

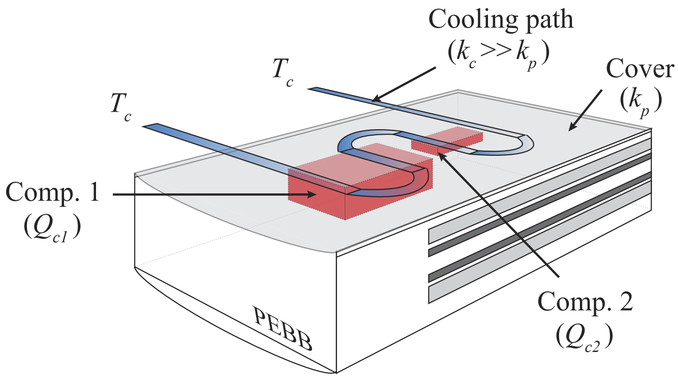

Fig. 8. Schematic of a serpentine cooling path layout on a PEBB 1000 [13].

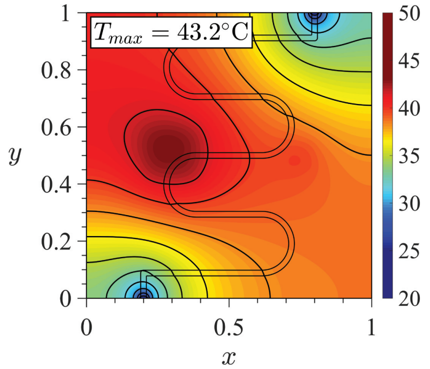

(a) Configuration 1

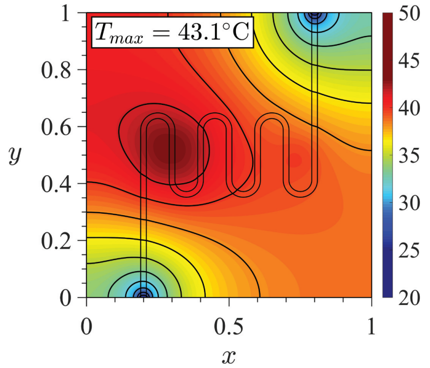

(b) Configuration 2

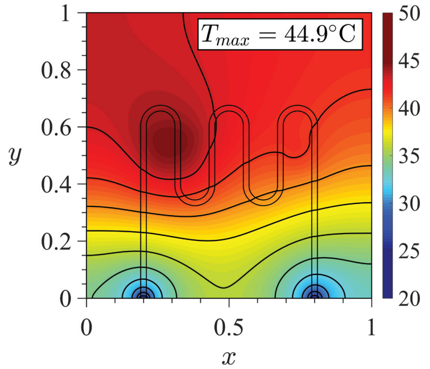

(c) Configuration 3

Fig. 9. PEBB cover temperature response to different serpentine cooling path layouts.

B. Optimized Heat Sink Topology

In addition to serpentine cooling paths, we optimized the topology of a high conductive heat sink extending from a cold end as depicted in Fig. 10, where $\tilde{k}$ is the thermal conductivity ratio between the heat sink and PEBB cover. The hot spot temperature across the PEBB cover was minimized in the optimization under a fixed heat sink volume, and high $\tilde{k}$ yielded a higher number of bifurcations as shown in Fig. 10 as more heat was transferred to the cold end per heat sink length.

The optimal topology is independent of the boundary temperature and heat generation rate as it solely depends on $\tilde{k}$, the available heat sink area, and the heat source location (uniform

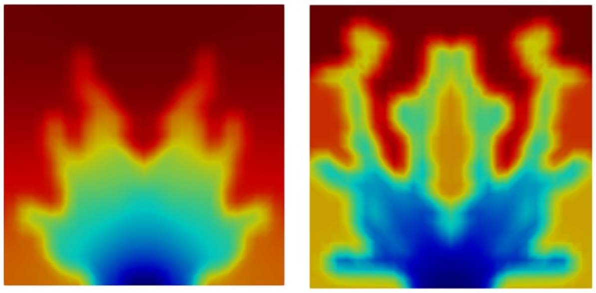

(a) $\tilde{k} = 100$ (b) $\tilde{k} = 1000$

Fig. 10. Optimized purely conductive heat sink topology.

or nonuniform). The results displayed in Fig. 10 are therefore valid for any system featuring the same objective function and design constraints. The color map in Fig. 10 represents a dimensionless temperature field whose absolute value will depend on the specific case. As with the serpentine cooling path, experimental validation of the developed heat sink model and an elaborate topology optimization study are underway.

C. Heat Pipes

The remarkably high heat dissipation rate of an envisioned PEBB 6000 would promote heat pipes as ideal candidates for effective cooling of localized hot spots. Owing to its extremely high effective thermal conductivity (≈ 100 times higher than pure copper) or low thermal resistance, heat pipes have been used extensively in electronics cooling [14] as heat spreaders as well as to enhance finned-heat sink performance. High performance heat pipe technologies with higher effective thermal conductivity and working heat fluxes have been demonstrated by developing innovative hybrid wicking structures as shown in Fig. 11.

The two hybrid wicking structure types in Fig. 11 have yielded improved heat pipe effectiveness in terms of thermal resistance reduction as depicted in Fig. 12. Therefore, custom designed heat pipes (hybrid wicking) can be used in a PEBB with variable heat loads over the surface. In addition to heat pipes, micro/mini channels can work effectively if the localized heat flux is very high. In cooling PEBB units, for instance, hot spots on chips can be selectively and effectively managed besides meeting the cooling requirements at modular level. Embedded microchannels can provide an effective cooling solution to these hot spots since silicon microchannels has been demonstrated to dissipate heat fluxes over 1 $\mathrm{kW/cm^2}$ [15]. Most recently, copper minichannels have also been shown to dissipate 1 $\mathrm{kW/cm^2}$ as shown in Fig 13, which provides a friendlier interface to current PEBB cooling designs.

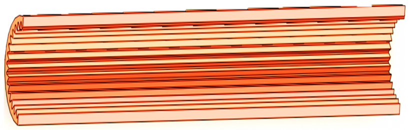

(a) Grooved

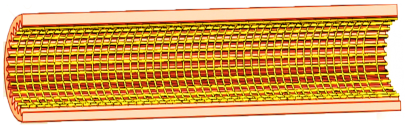

(b) Full hybrid

(c) Partial hybrid

Fig. 11. Heat pipes with three wicking structure types.

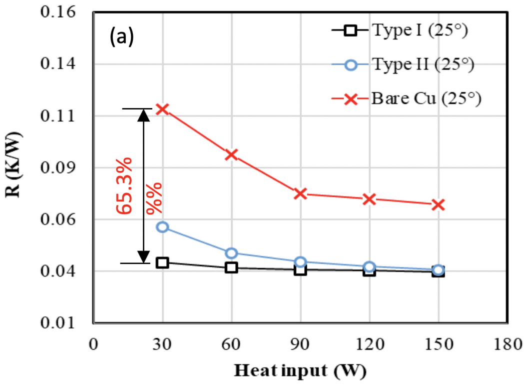

(a) 25°

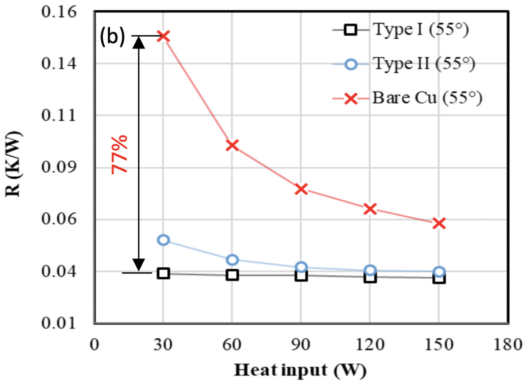

(b) 55°

Fig. 12. Effectiveness of hybrid wicking structures on heat pipe performance with respect to heat pipe tilt angle.

V. CONCLUSIONS

This paper considered several methods for cooling power electronics as applied to a PEBB 1000 and a notional PEBB 6000 under development at CPES/VT. Due to the early development status of the PEBB 1000 and PEBB 6000, neither experimental evaluation nor demonstration of any cooling strategy discussed in this paper has been performed; rather, this paper explores the calculations and other considerations used in selecting potential cooling strategies for further exploration. Preliminary numerical simulations (refer to Table II) indicate that air cooling is likely to be sufficient to meet the

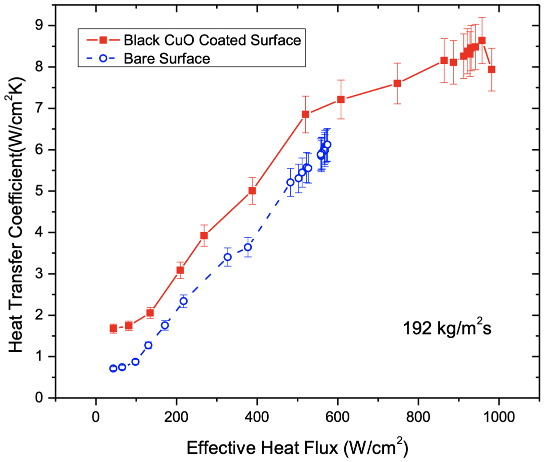

Fig. 13. Copper minichannel performance.

cooling needs of the PEBB 1000, as long as the internal heat sources are placed in direct contact with the thermal interfaces followed by optimized heat sink finned structures.

For the higher voltage/power PEBB units, air cooling, water cooling, and water cooling with a dry interface all have potential for meeting the cooling needs and warrant further investigation. In any case, the localized heat generated within the PEBB will require spreading to a larger surface area for subsequent transfer out of the PEBB. Having identified potential cooling strategies for PEBB 1000 and PEBB 6000, future work includes additional analysis to determine efficacy, efficiency, size and weight of the possible methods to include the impacts of both localized (PEBB-centric) structure and system-level structure of the cooling system options.

REFERENCES

[1] S. S. Murshed and C. N. De Castro, "A critical review of traditional and emerging techniques and fluids for electronics cooling," *Renewable and Sustainable Energy Reviews*, vol. 78, pp. 821–833, 2017.

[2] C. Cooke, C. Chryssostomidis, and J. Chalfant, "Modular integrated power corridor," in *2017 IEEE Electric Ship Technologies Symposium (ESTS)*. IEEE, 2017, pp. 91–95.

[3] C. DiMarino, I. Cvetkovic, Z. Shen, R. Burgos, and D. Boroyevich, "10 kV, 120 a SiC MOSFET modules for a power electronics building block (PEBB)," in *2014 IEEE Workshop on Wide Bandgap Power Devices and Applications*. IEEE, 2014, pp. 55–58.

[4] D. Boroyevich. CPES Research: SSPS–Building Blocks for the Future Electronic Power Grid. Virginia Tech. [Online]. Available: https://www.energy.gov/sites/prod/files/2017/09/f36/%5B7%5D%20VT%20-%20Dushan%20Boroyevich.pdf

[5] ——, "Use of SiC devices in medium-voltage converters," in *Proc. CPES Workshop WBG Power Electron. Adv. Distrib. Grids*, 2016.

[6] J. Wang, Z. Shen, and I. Cvetkovic, "Development of SiC-based PEBB 1000," Offline, Virginia Tech.

[7] K. Sheng, "Maximum junction temperatures of SiC power devices," *IEEE Transactions on Electron Devices*, vol. 56, no. 2, pp. 337–342, 2009.

[8] C. E. Green, V. Sahu, Y. Hu, Y. K. Joshi, and A. G. Fedorov, "Passive and active thermal technologies: Modeling and evaluation," *Handbook of 3D Integration: Design, Test, and Thermal Management*, vol. 4, pp. 375–412, 2019.

[9] M. M. Yovanovich and V. W. Antonetti, "Application of thermal contact resistance theory to electronic packages," *Advances in Thermal Modeling of Electronic Components and Systems*, vol. 1, pp. 79–128, 1988.

[10] A. Bejan and A. D. Kraus, *Heat transfer handbook*. John Wiley & Sons, 2003, vol. 1.

[11] M. M. Yovanovich, "Thermal interface (joint) conductance and resistance," in *ECE 309 Course Notes*, pp. 1–4.

[12] E. Fried, "Thermal conduction contribution to heat transfer at contacts," *Thermal conductivity*, vol. 2, pp. 253–274, 1969.

[13] H. C. Enriquez, S. Yang, and J. C. Ordonez, "Constructal theory of serpentines for the plate cooling with nonuniform heat generation," in *Constructal Law & Second Law Conference*, 2019.

[14] T. Yousefi, S. Mousavi, B. Farahbakhsh, and M. Saghir, "Experimental investigation on the performance of cpu coolers: effect of heat pipe inclination angle and the use of nanofluids," *Microelectronics Reliability*, vol. 53, no. 12, pp. 1954–1961, 2013.

[15] F. Yang, X. Dai, C.-J. Kuo, Y. Peles, J. Khan, and C. Li, "Enhanced flow boiling in microchannels by self-sustained high frequency two-phase oscillations," *International Journal of Heat and Mass Transfer*, vol. 58, no. 1-2, pp. 402–412, 2013.